

Effect of Sand Co-Presence on Cr^{VI} Removal in Fe⁰-H₂O System

Marius Gheju ^{1,*}  and Ionel Balcu ²

¹ Faculty of Industrial Chemistry and Environmental Engineering, Politehnica University Timisoara, Bd. V. Parvan Nr. 6, 300223 Timisoara, Romania

² National Institute for Research and Development in Electrochemistry and Condensed Matter, Str. Dr. Aurel Paunescu Podeanu Nr. 144, 300587 Timisoara, Romania

* Correspondence: marius.gheju@upt.ro; Tel.: +40-256-404185; Fax: +40-256-403060

Abstract: The aim of the present study was to provide new knowledge regarding the effect of non-expansive inert material addition on anionic pollutant removal efficiency in Fe⁰-H₂O system. Non-disturbed batch experiments and continuous-flow-through column tests were conducted using Cr^{VI} as a redox-active contaminant in three different systems: “Fe⁰ + sand”, “Fe⁰ only” and “sand only”. Both experimental procedures have the advantage that formation of (hydr)oxide layers on Fe⁰ is not altered, which makes them appropriate proxies for real Fe⁰-based filter technologies. Batch experiments carried out at pH 6.5 showed a slight improvement of Cr^{VI} removal in a 20% Fe⁰ system, compared to 50, 80 and 100% Fe⁰ systems. Column tests conducted at pH 6.5 supported results of batch experiments, revealing highest Cr^{VI} removal efficiencies for “Fe⁰ + sand” systems with lowest Fe⁰ ratio. However, the positive effect of sand co-presence decreases with increasing pH from 6.5 to 7.1. Scanning electron microscopy—energy dispersive angle X-ray spectrometry and X-ray diffraction spectroscopy employed for the characterization of Fe⁰ before and after experiments indicated that the higher the volumetric ratio of sand in “Fe⁰ + sand” system, the more intense the corrosion processes affecting the Fe⁰ grains. Results presented herein indicate the capacity of sand at sustaining the efficiency of Cr^{VI} removal in Fe⁰-H₂O system. The outcomes of the present study suggest that a volumetric ratio Fe⁰:sand = 1:3 could assure not only the long-term permeability of Fe⁰-based filters, but also enhanced removal efficiency of Cr^{VI} from contaminated water.

Keywords: metallic iron; hexavalent chromium; sand; water treatment



Citation: Gheju, M.; Balcu, I. Effect of Sand Co-Presence on Cr^{VI} Removal in Fe⁰-H₂O System. *Water* **2023**, *15*, 777. <https://doi.org/10.3390/w15040777>

Academic Editor: Andrea G. Capodaglio

Received: 31 January 2023

Revised: 10 February 2023

Accepted: 13 February 2023

Published: 16 February 2023



Copyright: © 2023 by the authors. Licensee MDPI, Basel, Switzerland. This article is an open access article distributed under the terms and conditions of the Creative Commons Attribution (CC BY) license (<https://creativecommons.org/licenses/by/4.0/>).

1. Introduction

Even though metallic iron (Fe⁰)-based water treatment technology was already applied for water potabilization in Europe around year 1890 at the water works of Antwerp (Belgium) [1], there has only been a growing interest in using Fe⁰ in remediation of contaminated water over the past three decades. Due to increasing industrial activities during the 20th century, water pollution has become a global issue of concern. Fe⁰ has been extensively applied, especially as reactive material in permeable reactive barriers (PRB), as a viable and cost-effective alternative for the conventional pump-and-treat technology, due to its low cost, widely availability and environmental friendliness; in addition, Fe⁰ is also very versatile and can be applied for the removal of various contaminants because it can act as adsorbent, reductant, as well as a generator of adsorbing, reducing and coagulation agents [2–5]. Both laboratory experiments and full-scale applications have warned that practical application (i.e., long-term operation) of Fe⁰-based filter treatment systems is impacted by the loss of filter hydraulic conductivity (caused by the expansive nature of iron corrosion products, mineral precipitation and gas formation that progressively fill the pore space within an Fe⁰-based filter) and loss of Fe⁰ efficiency caused by metal surface passivation, leading eventually to an incomplete utilization of Fe⁰ [6–10].

Theoretical studies published over the last several years concluded that mixing Fe⁰ with non-expansive additives (e.g., sand, pumice, etc.) could be a facile and efficient so-

lution for sustainable Fe⁰-based treatment systems [11–13]. By amending the reactive Fe⁰ with sand, several positive effects could be achieved, including (1) delayed filter clogging, (2) better pH control, (3) increased adsorption surface for contaminants, and (4) saving costs of water treatment systems [14–16]. However, a problem that may arise from “dilution” of Fe⁰ with sand is that, while having an undoubtful positive role on maintaining the long-term permeability of Fe⁰-based filters (i.e., enhancing the long-term sustainability), it may have a negative effect on pollutant removal percentages; to put it another way, while the “Fe⁰ only” filter can remove high percentages of pollutant (e.g., 100%), but only over a short time period (due to rapid clogging), the “Fe⁰ + sand” filter may have lower removal percentages (e.g., only 90%), but, instead, operates much longer (due to improved permeability). This behavior was observed at the very first Fe⁰-based PRB technology field demonstration, operated between 1991–1996 at Borden, Ontario, Canada [17], where constant removal efficiencies of only 90% and 86% were noticed over the duration of the test for trichloroethene and tetrachloroethene, respectively; not reaching 100% removal percentages was ascribed to the low mass ratio Fe⁰:sand in the reactive wall (22:78). However, it was presumed that the observed removal efficiency, although not being 100%, could have been maintained for at least another five years [16]. These results were later confirmed by continuous-flow experimental tests for Cu^{II}, Ni^{II} and Zn^{II} removal using columns filled with reactive mixtures comprising a fixed amount of Fe⁰ and various amounts of pumice in order to give 0–100% volumetric proportions of Fe⁰ [18]; the outcomes of this study showed that: (1) pollutant removal percentages were higher in the “Fe⁰-only” system, but only for a short duration because of the rapid clogging (after 17 days), and (2) the “Fe⁰ + sand” system was more sustainable than the “Fe⁰-only” system, with highest operational duration (90 days) observed for the lowest Fe⁰ proportion (10%). Therefore, even though it showed slightly lower removal percentages than the “Fe⁰-only” system, the “Fe⁰ + sand” system was the most efficient with respect to the total amount of metal removed per gram of Fe⁰ [18]. Similar outcomes were reported in another study [8] investigating removal of methylene blue (MB) via column experiments in “Fe⁰ only” system, and “Fe⁰ + sand” system with 30% (volume) Fe⁰; higher removal percentages and reduced operating time were observed for the “Fe⁰ only” system compared with higher operational duration and higher total amount of metal removed for the “Fe⁰ + sand” system [8]. Therefore, it is clear that a proper design of Fe⁰-based filters implies the careful consideration of a balance between acceptable removal efficiency and acceptable long-term hydraulic performance [8,16].

It must be noted here, however, that the Fe⁰-H₂O system is an ion-selective system with the highest affinity towards negatively charged pollutants [4,19]. The aforementioned studies have dealt with neutral [17] or cationic contaminants [8,18] with low affinity for the positively-charged (at circumneutral pH) iron (hydr)oxides covering the surface of Fe⁰. Thus, the question that arises is: what could be the influence of Fe⁰ “dilution” with sand on removal efficiency of anionic pollutants, and, particularly, of reducible anionic contaminants, in an Fe⁰-H₂O system? To obtain a reliable answer, only data provided by relevant experimental procedures that may be transferred to real Fe⁰-based filtration systems should be considered. It is well-known that in real Fe⁰-based filtration systems (e.g., PRBs) no intense mixing of the contaminated water with Fe⁰ exists; thus, (hydr)oxide film formation at the surface of Fe⁰ occurs with no disturbance [20]. However, most previous works studying contaminant removal in Fe⁰-H₂O systems were conducted under intensive mixing conditions (i.e., via well-mixed batch experiments), which result in mechanical abrasion of the surfaces and disturbance of (hydr)oxide film formation at the surface of Fe⁰ [21–40]; therefore, they will not be taken into further consideration in the present study, since they may report overestimated removal efficiencies of contaminants. As suggested by recent works [41,42], only non-disturbed (or very slowly) shaken batch experiments are appropriate for the investigation of contaminant removal in Fe⁰-H₂O systems; unfortunately, as far as we know, there are no studies regarding anionic contaminant removal in Fe⁰-H₂O systems conducted under such experimental conditions.

Even though well-designed batch experiments (i.e., non-disturbed or slowly shaken) can be useful in fine-tuning some relevant aspects at the laboratory scale, the most effective method of investigating the efficacy of Fe^0 filtration systems, which delivers experimental data with the best transferability to real water treatment systems (e.g., PRBs, SONO filters), is via flow-through column experiments [14,43–45]. To the best of our knowledge, to date, there are only a few such studies which may be considered for finding an answer to the aforementioned question. From the work of Westerhoff and James [43], it seems that a column packed with a mixture of 50% Fe^0 and 50% sand (*w:w*) (feed solution: 5–16 mg N/L; bed contact time: 1.5 h) was at least equally effective in removing NO_3^- as a column with 100% Fe^0 (feed solution: 2–5 mg N/L; bed contact time: 1.1 h); however, this conclusion is questionable since experimental conditions were not equal for the two columns. The study of Kaplan and Gilmore [46] specifically investigated, under continuous-flow conditions, the effect of sand co-presence on kinetics of Cr^{VI} removal with Fe^0 , reporting that varying the Fe^0 content in the column between 20 and 100% (weight) had no significant effect on the magnitude of the k_{obs} .

Therefore, the present study is aimed at providing new knowledge regarding the effect of sand co-presence on the efficiency of anionic contaminant removal in an Fe^0 - H_2O system. Cr^{VI} was selected as the model contaminant because, in addition to adsorption and co-precipitation which are the main mechanisms for neutral and cationic species removal in an Fe^0 - H_2O system, it can also be removed via reduction (predominantly indirect at circumneutral pH, by dissolved/bound/adsorbed Fe^{II}) to Cr^{III} followed by precipitation. To test the influence of sand co-presence on the efficiency of Cr^{VI} removal with Fe^0 , two experimental setups were employed: (1) non-disturbed batch experiments, and (2) continuous-flow-through column experiments. The extent of Cr^{VI} removal was comparatively discussed in three different systems: “ Fe^0 + sand”, “ Fe^0 only” and “sand only”; each system was characterized by the time-dependent changes of the Cr^{VI} , Cr^{III} , Fe^{II} and Fe^{III} concentration, as well as by the evolution of the pH.

2. Materials and Methods

2.1. Materials

Commercially available Fe^0 from Alfa Aesar (Ward Hill, MA, USA, $\geq 99\%$, size range 1–2 mm) was used as received. Sand from a local aquifer was washed with distilled water, air-dried at room temperature and sieved in the particle size range of 0.5–1.2 and 1.2–2.0 mm. A stock solution of Cr^{VI} (10 g/L) was prepared by dissolving 28.29 g of AR grade $\text{K}_2\text{Cr}_2\text{O}_7$ in 1000 mL of deionized water; then, working solutions of the desired initial Cr^{VI} concentration were prepared by diluting the stock solution. Natural (tap) water was used as background electrolyte to prepare the working solutions in order to simulate a freshwater contamination event; this was proven in numerous previous studies to be the best option for reproducing Fe^0 corrosion in natural waters [20,43,47].

2.2. Experimental Procedure

2.2.1. Non-Disturbed Batch Experiments

Non-disturbed batch tests were carried out using working solutions with pH 6.5 and Cr^{VI} concentrations of 5 and 100 mg/L for an experimental duration of 40 days. The two concentrations were chosen because they are within the range of levels reported for natural water environments polluted with low [48] and high [49] Cr^{VI} concentrations. Experiments were initiated by adding 20 mL working solution in assay tubes containing either: (1) Fe^0 + sand (1.2–2 mm), (2) Fe^0 only, or (3) sand (1.2–2 mm) only. Assay tubes were kept in darkness, at room temperature (23 ± 2 °C), throughout the duration of experiments. The volume of Fe^0 was fixed at 0.05 cm³ (0.2 g) and 1 cm³ (4 g) for tests with low (5 mg/L) and high (100 mg/L) Cr^{VI} concentration, respectively; this amount represented 100% of the reactive agent for the “ Fe^0 only” system. Three “ Fe^0 + sand” systems were tested: 20, 50 and 80% Fe^0 (volumetric proportions), prepared by mixing the fixed masses of Fe^0

with appropriate amounts of sand. The same mass ratios of $\text{Cr}^{\text{VI}}:\text{Fe}^0$, $\text{Cr}^{\text{VI}}:\text{Fe}^0:\text{sand}$ and $\text{Cr}^{\text{VI}}:\text{sand}$ were employed for both low and high Cr^{VI} concentration experiments.

2.2.2. Continuous-Flow-through Column Experiments

Column experiments were conducted in up-flow mode using vertical polyethylene columns of 12 cm height with 3 cm internal diameter. A 5 mg/L Cr^{VI} solution with pH 6.5 was pumped from the feed reservoir through the columns at a constant flow rate (30 mL/h) and room temperature (23 ± 2 °C) by an Ismatec IP08 peristaltic pump. From the bottom to the top, columns were packed with the following three layers (Figure 1): (1) sand (1.2–2.0 mm, $V_1 = 5.0$ cm³), (2) reactive zone (V_2), and (3) sand (0.5–1.2 mm, $V_3 = 5.0$ cm³).

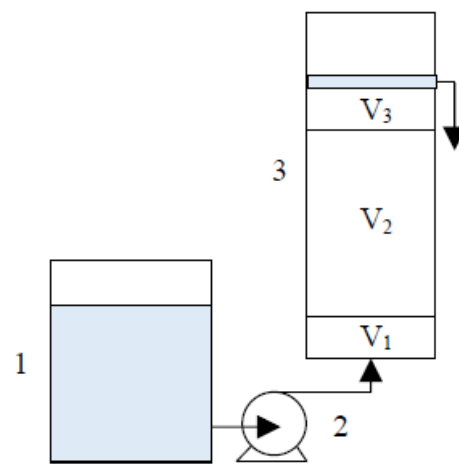


Figure 1. Column experimental setup: (1) Cr^{VI} solution storage tank; (2) peristaltic pump; (3) column with V_1 (sand 1.2–2.0 mm, 5.0 cm³), V_2 (reactive zone) and V_3 (sand 0.5–1.2 mm, 5.0 cm³) layers.

Three different systems were investigated: (1) Fe^0 + sand (1.2–2 mm), (2) Fe^0 only, and (3) sand only (1.2–2 mm). Two types of reactive zone (V_2) containing Fe^0 were explored:

(1) Reactive zone with fixed Fe^0 volume/mass (20 cm³/80 g) and variable total volume V_2 (20, 30, 40 and 60 cm³) (Figure 2). These reactive zones corresponded to the following Fe^0 volumetric percentages: (a) 100% (20 cm³ Fe^0 only), (b) 66.6% (mixture of 20 cm³ Fe^0 + 10 cm³ sand), (c) 50% (mixture of 20 cm³ Fe^0 + 20 cm³ sand), and (d) 33.3% (mixture of 20 cm³ Fe^0 + 40 cm³ sand). In addition, one control (0% Fe^0) column experiment was carried out with reactive zone V_2 containing only 60 cm³ sand. In order to investigate the influence of pH, an additional set of identical column experiments were conducted at pH 7.1.

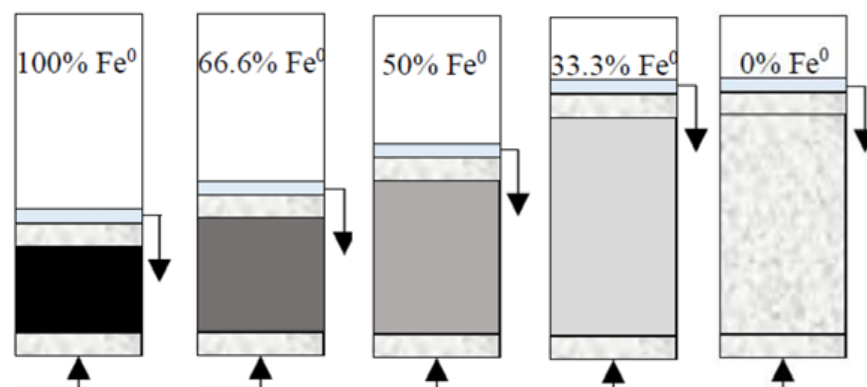


Figure 2. Experimental setup for column tests with reactive zone having fixed Fe^0 volume (20 cm³) and variable total volume V_2 (20, 30, 40 and 60 cm³). The control (0% Fe^0) column is also depicted.

(2) Reactive zone with variable Fe⁰ volume/mass (10 cm³/40 g, 20/80 g, 25 cm³/100 g, 30 cm³/120 g, 40 cm³/160 g and 50 cm³/200 g) and fixed total volume V₂ (50 cm³) (Figure 3). These reactive zones corresponded to the following Fe⁰ volumetric percentages: (a) 100% (50 cm³ Fe⁰ only), (b) 80% (mixture of 40 cm³ Fe⁰ + 10 cm³ sand), (c) 60% (mixture of 30 cm³ Fe⁰ + 20 cm³ sand), (d) 50% (mixture of 25 cm³ Fe⁰ + 25 cm³ sand), (e) 40% (mixture of 20 cm³ Fe⁰ + 30 cm³ sand) and (f) 20% (mixture of 10 cm³ Fe⁰ + 40 cm³ sand).

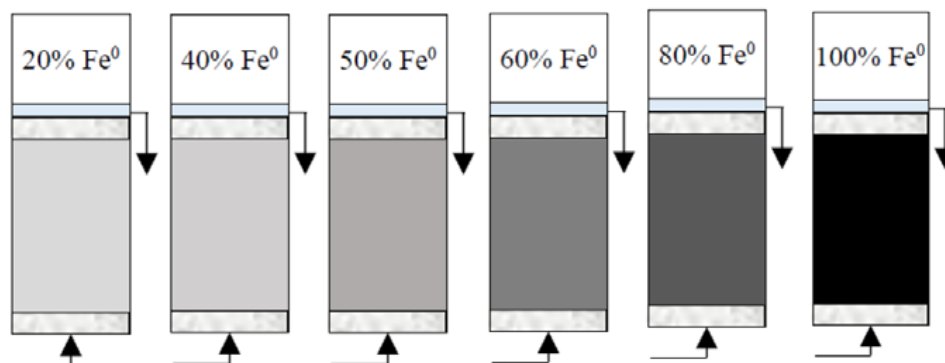


Figure 3. Experimental setup for column tests with reactive zone having variable Fe⁰ volume (10, 20, 25, 30, 40 and 50 cm³) and fixed total volume V₂ (50 cm³).

2.3. Analytical Procedure

Samples collected from batch and column tests were analyzed for Cr^{VI}, Cr^{total}, Fe^{II} and Fe^{total} via spectrophotometric methods using a Specord 200 PLUS spectrophotometer. Cr^{VI} concentration was determined by the 1,5-diphenylcarbazide method at 540 nm [50]; Cr^{total} was analyzed by oxidizing any Cr^{III} with KMnO₄, followed by analysis as Cr^{VI}. Then, Cr^{III}, if any, was evaluated as the difference between Cr^{total} and Cr^{VI}. Fe^{II} concentrations in the effluent were analyzed by the 1,10-orthophenanthroline method at 510 nm [51]. Fe^{total} was determined by reduction of any Fe^{III} to Fe^{II} with hydroxylamine hydrochloride, followed by analysis as Fe^{II}; Fe^{III} was determined from the difference between Fe^{total} and Fe^{II}. An Inolab 7320 pH-meter calibrated with three standards was used to measure the pH. All represented data are the mean values of two experimental replicates.

X-ray diffraction (XRD) and scanning electron microscopy (SEM)—energy dispersive angle X-ray spectrometry (EDX) were employed to investigate the chemical composition and surface morphology of both fresh and exhausted Fe⁰ from batch experiments with high Cr^{VI} concentration. SEM-EDX analysis was performed on an Inspect S scanning electron microscope (FEI, Holland) coupled with a GENESIS XM 2i energy dispersive angle X-ray spectrometer to obtain the atom composition. XRD measurements were performed at 40 kV and 30 mA on an X'Pert PRO MPD Diffractometer (FEI, Holland) equipped with a Cu anode X-ray tube and PixCEL detector (Cu K α radiation, $\lambda = 1.54056 \text{ \AA}$).

3. Results and Discussion

3.1. Solid Phase Characterization

To ensure conciseness of this article, the results of SEM-EDX and XRD analysis are discussed only for the 20, 50 and 100% Fe⁰ system. Analysis of exhausted Fe⁰ SEM images (Figures S2–S4) reveals the occurrence of typical amorphous structures, attributable to secondary mineral phases (iron corrosion products), which did not exist on the fresh Fe⁰ surface (Figure S1). Furthermore, SEM micrographs also indicate that the highest amount of secondary mineral phases were formed at the surface of exhausted Fe⁰ from the 20% Fe⁰ system (Figure S4), while much lower quantities were observed at the surface of 50 and 100% Fe⁰ systems (Figures S2 and S3).

The EDX spectrum of exhausted Fe⁰ from all investigated systems (Figures S6–S8) showed the appearance of additional chromium peaks, which did not exist for fresh Fe⁰ (Figure S5), indicating the retaining of chromium on the Fe⁰; in addition, it was noticed

that more intense chromium peaks were observed for the 20% Fe⁰ system, compared to the 50 and 100% Fe⁰ systems. Furthermore, EDX analysis also revealed a much greater oxygen content at the surface of exhausted Fe⁰ from the 20% Fe⁰ system, than at the surface of exhausted Fe⁰ from the 50 and 100% Fe⁰ systems. All this data strongly support the results of SEM analysis, indicating that the highest amount of iron corrosion products (Fe (hydr)oxides) existed at the surface of exhausted Fe⁰ from the 20% Fe⁰ system.

Analysis of the XRD diffractograms show that apart from the two peaks at 2θ values of 45° and 65° exhibited by fresh Fe⁰ [52] (Figure S9) no additional diffraction signals of other components were identified in the XRD pattern of exhausted Fe⁰ from the “Fe⁰ only” and the “Fe⁰ + sand” systems (Figures S10–S12); this could be attributed to the fact that secondary mineral phases occurred at the surface of exhausted Fe⁰ in minor amounts and/or in amorphous form. However, the intensity of the Fe⁰ peak at the 2θ value of 65° was significantly decreased for the exhausted Fe⁰ in comparison to fresh Fe⁰, attributable to the occurrence of iron corrosion products at the surface of exhausted Fe⁰; moreover, it was noticed that the higher the percentage of sand in the “Fe⁰ + sand” system, the lower the intensity of the 65° peak.

To sum up, the results of solid phase characterization clearly indicate that amending Fe⁰ with sand results in more intense corrosion processes affecting the Fe⁰ grains; the higher the volumetric ratio of sand in the “Fe⁰ + sand” system, the higher the amount of iron corrosion products generated.

3.2. Non-Disturbed Batch Tests

The influence of sand co-presence on Cr^{VI} removal with Fe⁰ in a non-disturbed batch system is depicted in Figures 4 and 5. It is apparent from these figures that after 40 days no significant differences can be perceived between the 100% Fe⁰, the 80% Fe⁰ and the 50% Fe⁰ systems for both types of experiments. Instead, slightly better removal efficiencies of Cr^{VI} were noticed for the 20% Fe⁰ system than for systems with 50–100% Fe⁰. This is in agreement with results presented at Section 3.1, indicating that the most intense Cr EDX peaks were observed for the exhausted Fe⁰ from the 20% Fe⁰ system. It is important to note that the improvement of Cr^{VI} removal in the 20% Fe⁰ system was observed only after about 30 days of the experiment when important amounts iron corrosion products were already generated; this reveals the importance of iron corrosion products for the mechanism of Cr^{VI} removal.

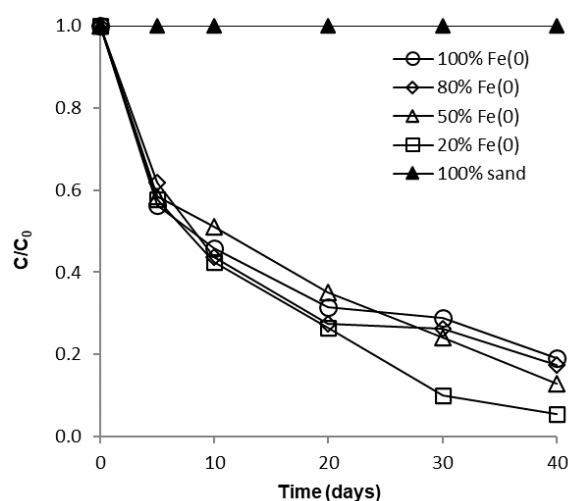


Figure 4. Time profile of Cr^{VI} removal for batch experiments at low initial concentration.

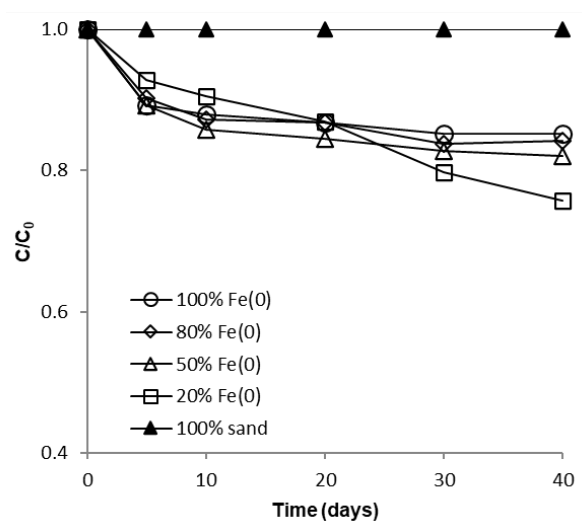
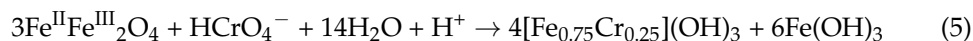
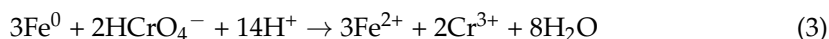


Figure 5. Time profile of Cr^{VI} removal for batch experiments at high initial concentration.

Since the same Cr^{VI}: Fe⁰ mass ratio was applied in both types of tests (with low and high Cr^{VI} concentration), another important outcome that clearly results from analysis of Figures 4, 5 and S13 is the fact that removal of Cr^{VI} with Fe⁰ was severely hindered by the increase of Cr^{VI} concentration, not only in the “Fe⁰ only”, but also in the “Fe⁰ + sand” system; this is in opposition to recent findings revealing that comparable removal efficacies were achieved both at low and high Cr^{VI} concentration in the “Fe⁰ + MnO₂” system [47]. Therefore, it was revealed by the non-disturbed batch experiments that the ability of sand to improve the removal of Cr^{VI} with Fe⁰ is much lower than that of MnO₂.

No Cr^{VI} removal was observed in the “sand only” system, in accord with earlier findings reporting that sand has no ability in adsorbing Cr^{VI} [46]. Dissolved Fe^{II} was not detected in the supernatant, regardless of type of experiment, which indicates that all Fe^{II} resulting from the Fe⁰ corrosion process was subsequently involved in: (1) indirect reduction of Cr^{VI}, (2) precipitation as a condensed phase of (oxy)hydroxides, and (3) oxidation to Fe^{III} and subsequent precipitation as a condensed phase of (oxy)hydroxides. Dissolved Fe^{III} and Cr^{III} were also not identified in the supernatant, attributable to their (co-)precipitation as simple or/and mixed Fe^{III}–Cr^{III} (oxy)hydroxides, a process that occurs at pH > 4 [53].

Over the course of batch experiments, pH increased from 6.5 to 7.5–7.7 and 7.4–7.5 for tests at low and high Cr^{VI} concentration, respectively (Figures 6 and 7); the increase was more rapid for experiments at low Cr^{VI} concentration and rather sequential for tests at high Cr^{VI} concentration. No significant differences were observed between the final pH values (after 40 days) in the “Fe⁰ + sand” and the “Fe⁰ only” system. The pH increase was the result of: (1) HO⁻ generation in Fe⁰ oxidative dissolution processes (Equations (1) and (2)), mainly due to oxidation with water, and (2) H⁺ consuming reactions (Equations (3)–(5)), mainly due to indirect reduction of Cr^{VI} with dissolved or solid Fe^{II}-based corrosion products [54].



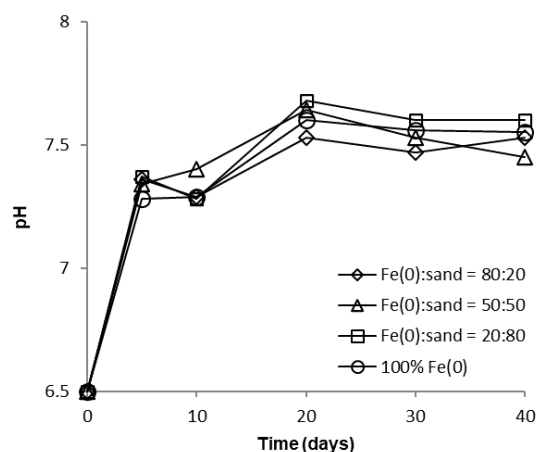


Figure 6. Evolution of pH in batch experiments at low Cr^{VI} initial concentration.

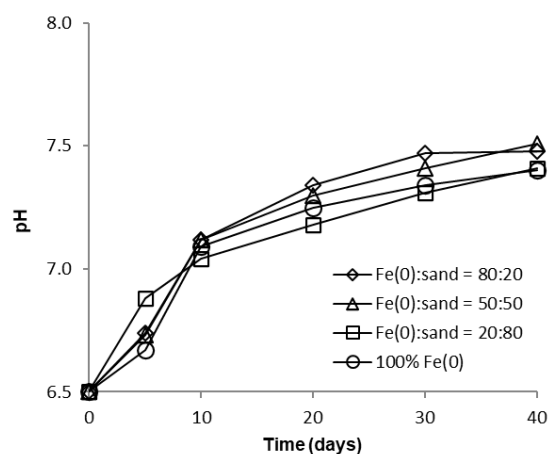


Figure 7. Evolution of pH in batch experiments at high Cr^{VI} initial concentration.

However, passivation of the Fe^0 surface with solid mineral phases (mainly Fe (oxy)hydroxides) will cause a decrease in Fe^0 corrosion rates and, eventually, limit the pH increase, as can be seen from Figures 6 and 7.

At this point, it should be recalled that mixing Fe^0 with non-expansive materials (e.g., sand) was suggested as a tool to increase the long-term hydraulic conductivity of Fe^0 beds [18,55]. So far, the present batch experiments suggest that a minor improvement of Cr^{VI} removal efficiency could also be achieved in an “ Fe^0 + sand” system, but only for the 20% Fe^0 system. In order to further investigate the effect of sand co-presence on removal efficacy of Cr^{VI} , additional continuous-flow-through column experiments were carried out, and the results are discussed in the following sections.

3.3. Cr^{VI} Evolution in Column Tests

3.3.1. Column Tests with Reactive Zone Having a Fixed Fe^0 Volume and Variable Total Volume V_2

The evolution of Cr^{VI} removal in column experiments with a fixed Fe^0 volume and variable total volume of the reactive zone is presented in Figure 8 and Figure S14. No Cr^{VI} removal was noticed in the “sand only” (0% Fe^0) control system over the entire duration of the experiment, in concordance with results of non-disturbed batch experiments. In columns with an Fe^0 -based reactive zone, Cr^{VI} breakthrough occurred after 2 days in the 100% Fe^0 system, 1 day in the 66.6% Fe^0 system, and from the very first day of the experiment in the 50% and 33.3% Fe^0 systems (Figure S14). Hence, it is obvious that mixing sand with Fe^0 in the reactive zone has a negative effect on the breakthrough time. Therefore, so far, it could be presumed that the co-presence of sand inside the reactive zone may have

a detrimental effect also on the efficiency of Cr^{VI} removal with Fe⁰. After the breakthrough, Cr^{VI} concentration continuously increased in all Fe⁰ based systems until reaching a quasi-steady-state concentration after about 70 days. The order of Cr^{VI} steady-state concentration value, which resulted from this study is: 100% Fe⁰ system > 50% Fe⁰ system ≈ 66.6% Fe⁰ system > 33.3% Fe⁰ system. Thus, there was no direct dependence between the value of Cr^{VI} steady-state concentration and the volumetric ratio of Fe⁰ in the reactive zone; while the lowest Cr^{VI} steady-state concentration was observed for the 33% Fe⁰ system, the highest Cr^{VI} steady-state concentration was noted for the 100% Fe⁰ system.

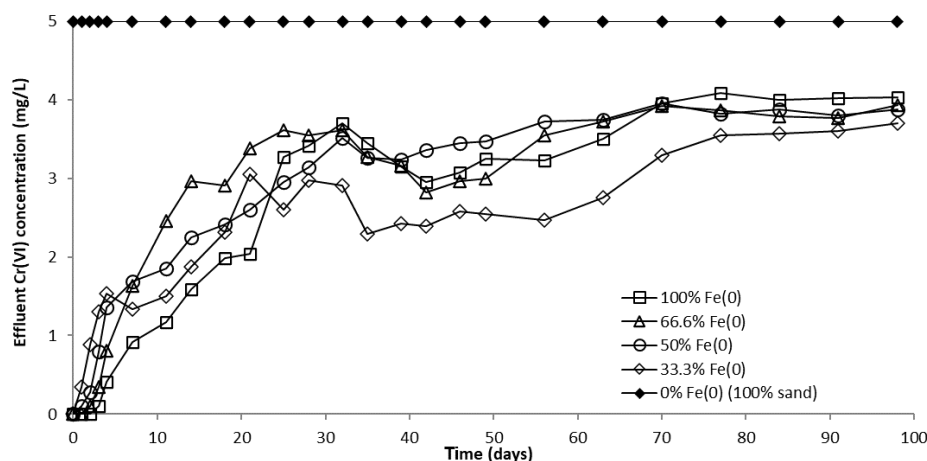


Figure 8. Cr^{VI} concentration in column effluent vs. time for columns having fixed Fe⁰ volume and variable total reactive zone volume V₂ at initial pH 6.5.

However, a comparison of the capacity of “Fe⁰ only” and “Fe⁰ + sand” systems to remove Cr^{VI} adds other important information, which counterbalances the aforementioned presumption. It can be seen from Figure 9 that the highest total Cr^{VI} removal capacity was observed for the 33% Fe⁰ system. The 100% Fe⁰ system exhibited the second best total Cr^{VI} removal capacity, higher than columns with 50% and 66.6% Fe⁰, but lower than the 33.3% Fe⁰ system. Therefore, it clearly results from these experiments that even though the 33.3% Fe⁰ system exhibited the fastest Cr^{VI} breakthrough, it displays the highest total Cr^{VI} removal capacity; this can be ascribed to the fact that the 33.3% Fe⁰ system showed the lowest value of Cr^{VI} in column effluent from day 25 till the end of the experiment. This behavior may be important, for instance, when treated water is blended in a certain proportion with clean water from a different source, and typical quality regulations are still achieved for the resulting mixed water in spite of Cr^{VI} breakthrough in the treated water.

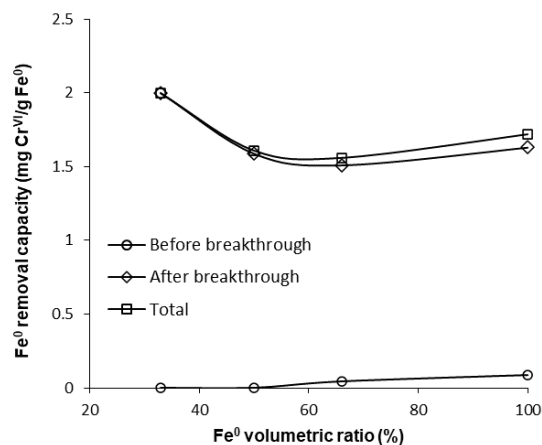


Figure 9. Cr^{VI} removal capacity of Fe⁰ at pH 6.5 for columns having fixed Fe⁰ volume and variable total reactive zone volume V₂.

Finding the 33.3% Fe⁰ column to be the most efficient Fe⁰-based system, in terms of mass of Cr^{VI} removed per mass unit of Fe⁰, is in correlation with results of previous studies indicating that to be sustainable an Fe⁰-based filter should contain less than 60% (vol) Fe⁰, ideally 25% [8,56–58].

In order to investigate the influence of pH, an identical column experiment was conducted using a Cr^{VI} solution with pH 7.1. The results presented in Figure 10 and Figure S15 reveal that the Cr^{VI} breakthrough occurred after 1 day in 100% and 66.6% Fe⁰ systems, while in 50% and 33.3% Fe⁰ systems, Cr^{VI} breakthrough was observed from the very first day of the experiment. After breakthrough, the concentration of Cr^{VI} in column effluents increased until a steady-state concentration was reached after about 40 days. The order of the Cr^{VI} steady-state concentration value was: 50% Fe⁰ system > 66.6% Fe⁰ system ≈ 33.3% Fe⁰ system > 100% Fe⁰ system. Therefore, the highest Cr^{VI} steady-state concentration at pH 7.1 was noted for the 50% Fe⁰ system, while the lowest was noted for the 100% Fe⁰ system, in contrast to experiments at pH 6.5, where highest and lowest Cr^{VI} steady-state concentration were observed for the 100% and 33.3% Fe⁰ system, respectively.

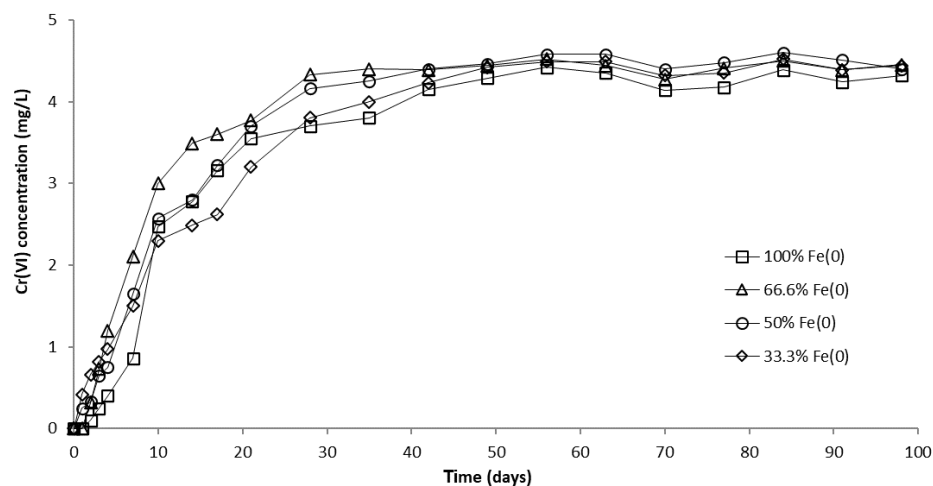


Figure 10. Cr^{VI} concentration in column effluent vs. time for columns having fixed Fe⁰ volume and variable total reactive zone volume V_2 at initial pH 7.1.

All these observations could suggest that the co-presence of sand inside the reactive zone could have a detrimental effect at pH 7.1. However, from the comparison of the capacity of the “Fe⁰ only” and the “Fe⁰ + sand” systems to remove Cr^{VI} (Figure 11), it can be seen that at pH 7.1 the 33.3% and 100% Fe⁰ systems exhibited similar total Cr^{VI} removal capacities. By gradually increasing the Fe⁰ ratio from 33% to 50% and to 66.6%, a decrease in total Cr^{VI} removal capacity was noted. Therefore, even though the 33.3% Fe⁰ system exhibited the fastest Cr^{VI} breakthrough, it displays a comparable Cr^{VI} total removal capacity to the 100% Fe⁰ system; this can be attributed mainly to the low rate of Cr^{VI} concentration increase observed for the 33.3% Fe⁰ system during the first 40 days following the breakthrough.

Cr^{VI} breakthrough time in the 100% Fe⁰ system was lower at pH 7.1 (1 day) than at 6.5 (2 days), and Cr^{VI} breakthrough concentrations were higher at pH 7.1 than at 6.5 (Figures S14 and S15). In addition, faster rates of Cr^{VI} concentration increase after breakthrough, and higher values of steady-state Cr^{VI} concentration were noted at pH 7.1 than at 6.5 (Figures 8 and 10). Furthermore, by comparing the values of Cr^{VI} removal capacities (Figures 9 and 11), it can be seen that an increase in pH from 6.5 to 7.1 leads to a reduced Cr^{VI} removal efficiency in both the “Fe⁰ only” and the “Fe⁰ + sand” systems. While it is well-known that efficiency of Cr^{VI} removal with Fe⁰ decreases with increasing pH [54], the present experiments suggest that the magnitude of the positive effect of sand co-presence also decreases with increasing pH from 6.5 to 7.1.

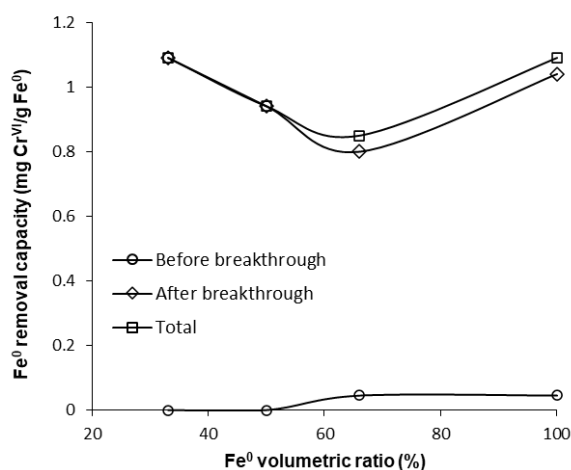


Figure 11. Cr^{VI} removal capacity of Fe⁰ at pH 7.1 for columns having fixed Fe⁰ volume and variable total reactive zone volume V_2 .

The higher Cr^{VI} breakthrough concentrations, faster rates of Cr^{VI} concentration increase after breakthrough and higher values of steady-state Cr^{VI} concentration observed at pH 7.1 than at pH 6.5 can be ascribed to: (1) lower proton concentration at pH 7.1 than at 6.5, which from a thermodynamic standpoint hinders reduction of Cr^{VI}, (2) lower amounts of Fe^{II} generated as a result of lower rates of Fe⁰ corrosion at pH 7.1 than at 6.5, and (3) lower amounts of dissolved Fe^{II} existent in solution due to the scavenging of generated Fe^{II} by the surface of the sand and of Fe⁰ via adsorption, precipitation and oxidation to Fe^{III}; this means that lower amounts of dissolved Fe^{II} are available for homogeneous indirect reduction of Cr^{VI}. Obviously, all mentioned Fe^{II} competitive processes occur both at pH 6.5 and 7.1. However, it must be recalled that efficiency of both Fe^{II} adsorption and precipitation processes increases with increasing solution pH. Moreover, it is well-known that the rate of Fe^{II} oxidation by dissolved O₂ (existent in our tap water in a concentration of about 7 mg/L) also significantly increases with pH [59–62]. Therefore, the efficiency of all mentioned Fe^{II} competitive processes is higher at pH 7.1 than at pH 6.5.

3.3.2. Column Tests with Reactive Zone Having Variable Fe⁰ Volume and Fixed Total Volume V_2

The evolution of Cr^{VI} removal in column experiments with variable Fe⁰ volume and fixed volume of total reactive zone is depicted in Figure 12, Figure 13 and Figure S16. It can be clearly seen from these images that the higher the volume (mass) of Fe⁰ within the reactive zone, the longer the breakthrough times and the higher the Cr^{VI} removal efficiencies. This is consistent with results of previous studies indicating that increasing the mass of Fe⁰ has a favorable effect on Cr^{VI} removal efficiency due to an increased Fe⁰ surface area and thus, a proportionally greater number of reactive sites available for removal of Cr^{VI} [54].

For columns packed with a reactive zone containing 50–100% Fe⁰, Cr^{VI} concentration increased after breakthrough until a steady-state concentration was observed; the higher the volumetric percentage of Fe⁰ in the reactive zone, the lower the value of steady-state Cr^{VI} concentration. Instead, for columns packed with a reactive zone containing 20% and 40% Fe⁰, Cr^{VI} concentration continuously increased after breakthrough until the initial concentration of 5 mg/L was reached, and no steady-state concentration was observed; this behavior is attributable to the low amount of Fe⁰ in the reactive zone.

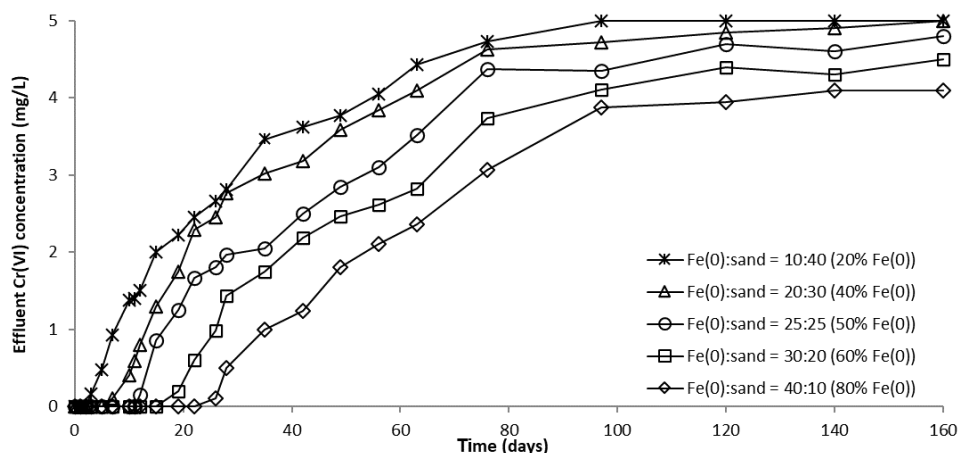


Figure 12. Cr^{VI} concentration in column effluent vs. time for columns with “Fe⁰ + sand” reactive zone having variable Fe⁰ volume and fixed total volume V₂.

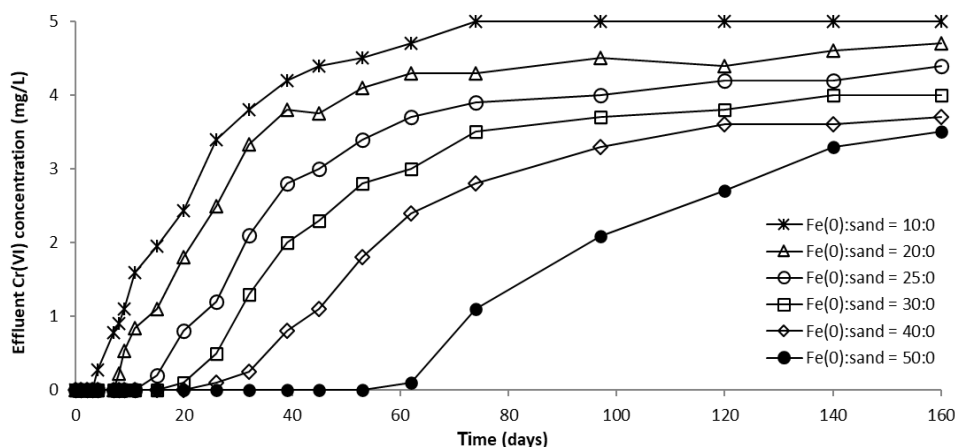


Figure 13. Cr^{VI} concentration in column effluent vs. time for control columns packed with “Fe⁰ only” reactive zone.

Furthermore, Figure 12, Figure 13 and Figure S16 also reveal that Cr^{VI} breakthrough occurred faster for the “Fe⁰ + sand” system than for the “Fe⁰ only” control system; the only exception was represented by column experiments with 40 cm³ Fe⁰, when Cr^{VI} breakthrough took place almost simultaneously for the “Fe⁰ + sand” and the “Fe⁰ only” systems. This confirms the results obtained in column tests with a reactive zone having fixed Fe⁰ volume and variable total volume V₂ (Figures 8 and 10), supporting the conclusion that the co-presence of sand inside the reactive zone shortens the duration of the period when the column operates with no Cr^{VI} detected in the effluent. However, a comparison of the total capacity of the “Fe⁰ only” and the “Fe⁰ + sand” system to remove Cr^{VI} (Figure 14) reveals that the highest total Cr^{VI} removal capacity was observed for the lowest Fe⁰ volumetric ratio in the reactive zone (i.e., 20% Fe⁰). Subsequently, by increasing the Fe⁰ volumetric ratio to 40%, an important decrease in total removal capacity was noted, which was also maintained quasi-constant when the Fe⁰ volumetric ratio was further increased up to 80%. Finally, an increase in total removal capacity was perceived for the column packed with 100% Fe⁰; however, total removal capacity of the 100% Fe⁰ system was lower than the 20% Fe⁰ system. This corroborates the results obtained in column tests with reactive zone having fixed Fe⁰ volume and variable total volume V₂ (Section 3.3.1), revealing that a water treatment filter with 20–33% Fe⁰ volumetric ratio in the “Fe⁰ + sand” reactive zone could be more efficient for removal of Cr^{VI} than a 100% Fe⁰ system.

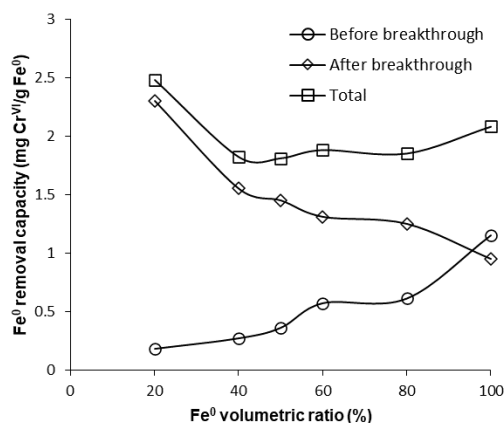


Figure 14. Cr^{VI} removal capacity of Fe⁰ for columns having variable Fe⁰ volume and fixed total volume V_2 .

Column experiments carried out in this study confirmed the results of the non-disturbed batch test indicating that sand has no ability to retain Cr^{VI}; hence, the elevated removal efficiencies observed for the “Fe⁰ + sand” systems with the highest volumetric percentage of sand and the lowest of Fe⁰ cannot be attributed to Cr^{VI} adsorption on sand. There are, instead, several other effects of sand that may have caused this result: (1) sand can be regarded as a dispersant material, sustaining the system’s efficiency by avoiding/delaying the cementation/compaction of Fe(OH)_n colloids, thus avoiding/delaying the porosity loss of the column reactive zone [41,63]; (2) sand helps expose more Fe⁰ surface to aqueous Cr^{VI} solution [64]; (3) for a fixed amount of Fe⁰, the volume of the reactive zone increases as a result of mixing Fe⁰ with sand; accordingly, higher hydraulic retention times will be recorded in “Fe⁰ + sand” than in “Fe⁰ only” system [10]; (4) sand offers a supplementary surface for precipitation of cations resulting from Fe⁰ corrosion, thus diminishing rates of Fe⁰ surface passivation [65]; (5) since Fe^{II}-bearing minerals precipitated on sand are not only good adsorbents for Cr^{VI}, but also stronger reductants than dissolved Fe^{II} [66], they are able to remove Cr^{VI} by a rapid adsorption–reduction mechanism [67]; and (6) Fe^{II} adsorbed on mineral surfaces (e.g., montmorillonite, kaolinite, α -FeOOH, γ -FeOOH, SiO₂) has a higher tendency to reduce Cr^{VI} than dissolved Fe^{II} [68,69].

Effects (3), (4), (5) and (6) exerted by sand support the conclusion that the most important path of Cr^{VI} removal with Fe⁰ was the indirect reduction with Fe^{II} corrosion products (dissolved Fe^{II} and Fe^{II}-bearing secondary minerals) [47]. This agrees with previous reports [46] that ascribed the lack of dependency of the Cr^{VI} depletion rate constants on the Fe⁰ percentage in the column to the removal of Cr^{VI} via adsorption and reduction (with Fe^{II}) processes. Therefore, our results confirm the importance of adsorption and indirect reduction within the mechanism of Cr^{VI} removal with Fe⁰, in concordance with a recently postulated concept trying to revise the mechanism of contaminant removal in an Fe⁰-H₂O system. As stated by this new concept, under environmental relevant pH values, Fe⁰ should be regarded mainly as the generator of removing agents (adsorbents/coagulants/reductants); accordingly, removal of contaminants with Fe⁰ occurs primarily due to adsorption/co-precipitation/size filtration processes, while contaminant reduction, when applicable, mostly results from indirect reducing agents and should be regarded as a parallel reaction of aqueous Fe⁰ corrosion [2,20,70,71].

3.4. pH Evolution in the Column Tests

The evolution of pH in column effluents is presented in Figures 15–17. It can be seen that at the beginning of the experiment, Cr^{VI} removal was accompanied by an increase in pH; Fe⁰ corrosion and Cr^{VI} reduction are responsible for this pH change, both processes involving the consumption of protons. Subsequently, the pH dropped until it reached a steady-state value, attributable to Fe⁰ surface passivation, which causes a decline in Fe⁰ corrosion.

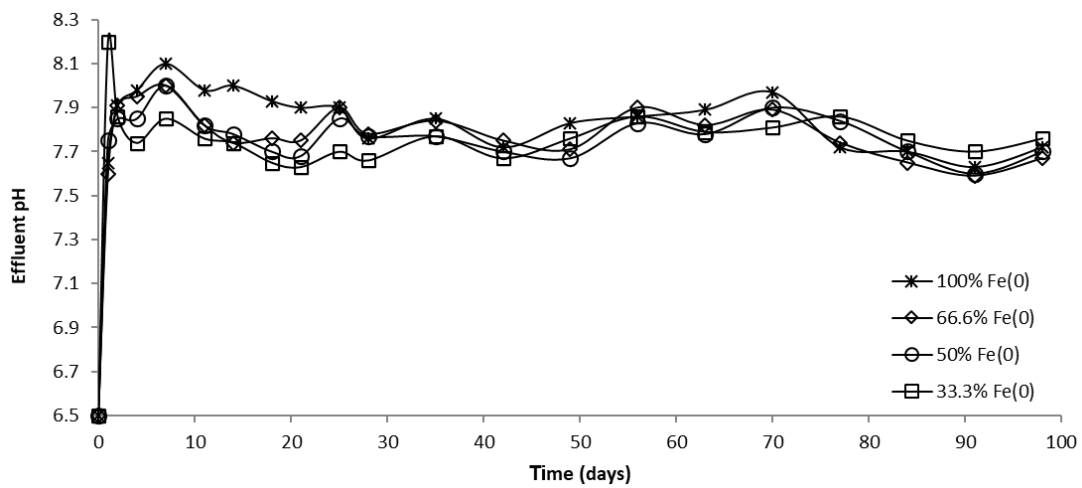


Figure 15. The pH in column effluent vs. time for columns having fixed Fe⁰ volume and variable total reactive zone volume V₂ at initial pH 6.5.

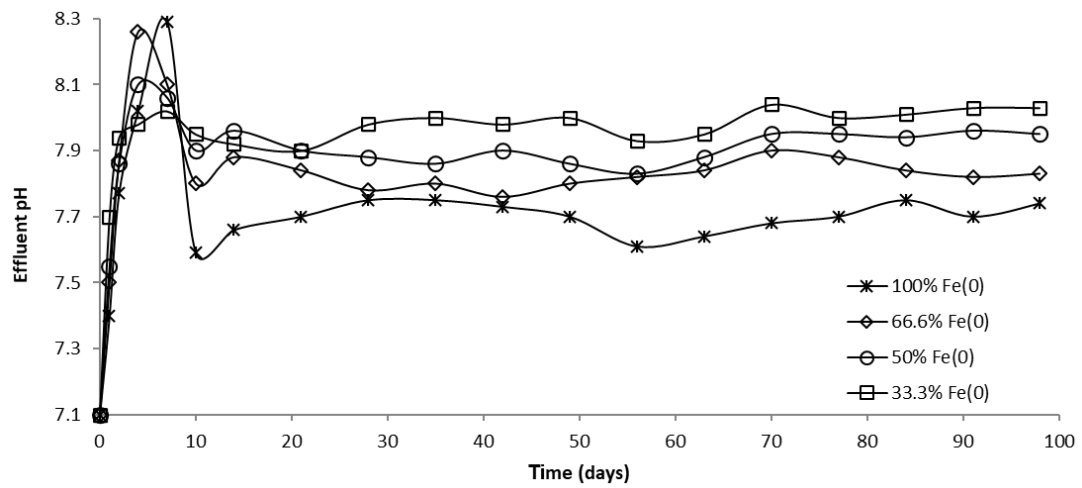


Figure 16. The pH in column effluent vs. time for columns having fixed Fe⁰ volume and variable total reactive zone volume V₂ at initial pH 7.1.

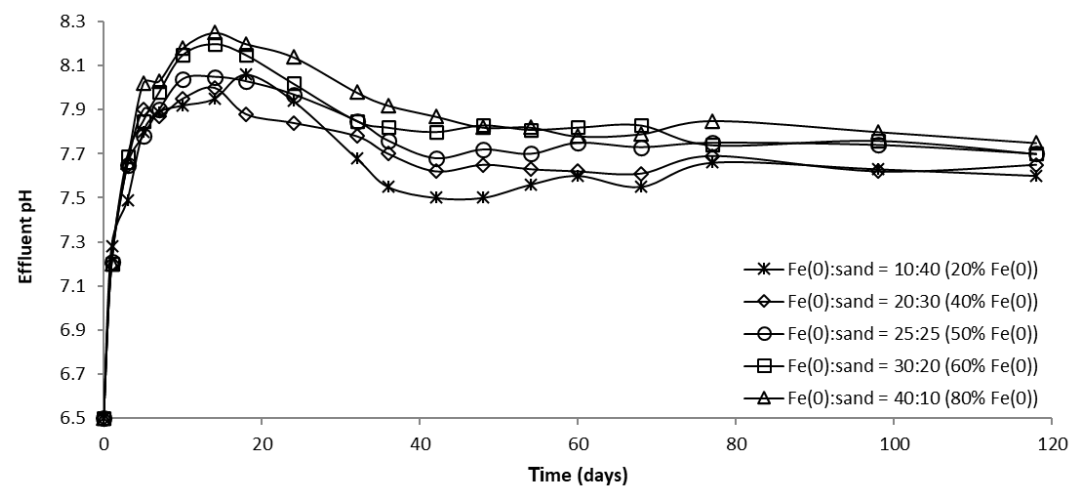


Figure 17. The pH in column effluent vs. time for columns having variable Fe⁰ volume and fixed total reactive zone volume V₂.

3.5. Cr^{III} , Fe^{III} and Fe^{II} Evolution in Column Tests

The presence of Cr^{III} , Fe^{III} and Fe^{II} in column effluent was investigated in column experiments having fixed Fe^0 volume and a variable total reactive zone volume V_2 . No dissolved Fe^{III} and Cr^{III} was detected in column effluent, regardless of the type of experiment, which suggests that it was all retained inside the column via adsorption and (co-)precipitation. Small amounts of dissolved Fe^{II} were determined in column effluent at the beginning of the experiments conducted at pH 6.5; instead, at pH 7.1, no dissolved Fe^{II} was found, which suggests that all Fe^{II} was retained (precipitated/adsorbed/oxidized to Fe^{III} and precipitated) inside the reactive zone.

The evolution of aqueous Fe^{II} concentration in column effluent as a function of elapsed time is presented in Figure 18. A rapid increase in iron concentration was noted during the first days of the experiment, followed by a rapid decrease in the following days. Since the main source of Fe^{II} species in column effluent is the Fe^0 corrosion process (Equations (1) and (2)), the decrease in Fe^{II} concentration with increasing experimental time can be attributed to passivation of the Fe^0 surface with solid iron (hydr)oxides, which lowers corrosion rates. Another important conclusion that can be drawn from Figure 18 is that higher Fe^{II} concentrations were observed in the effluent of the “ Fe^0 only” system than in the “ Fe^0 + sand” system, which is strong evidence of the ability of sand to retain Fe^0 corrosion products.

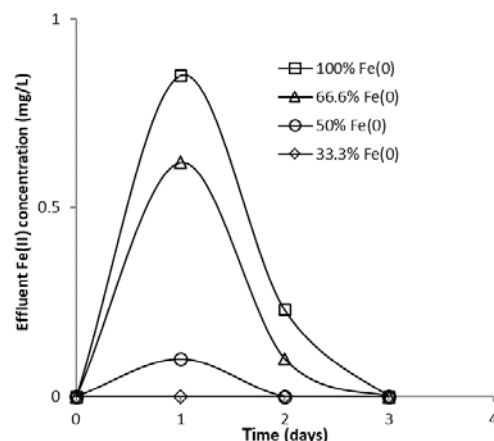


Figure 18. Fe^{II} concentration in column effluent vs. time for columns having fixed Fe^0 volume and variable total reactive zone volume V_2 at initial pH 6.5.

The faster Cr^{VI} breakthrough observed at both pH 7.1 and 6.5 for the “ Fe^0 + sand” system compared to the “ Fe^0 only” system can be attributed to scavenging of Fe^{II} by sand via adsorption and precipitation processes followed by possible oxidation to Fe^{III} . Section 3.3 shows that the solution pH inside the column was alkaline, which favors adsorption and/or precipitation of Fe^{II} at the surface of the sand and its subsequent oxidation to Fe^{III} . This is in accord with results of previous studies reporting that adsorption of dissolved Fe^{II} on minerals (sand, iron oxide coated sand, calcite) is enhanced at higher pH, while subsequent oxidation of adsorbed Fe^{II} with dissolved O_2 is catalyzed by the mineral surface and by the high pH [72–75]. Thus, it seems that dissolved Fe^{II} had the most important role in removal of Cr^{VI} (via homogeneous reduction to Cr^{III}) at the beginning of the experiments, while solid Fe^{II} / Fe^{III} -bearing secondary minerals were the major Cr^{VI} removal agents (via reduction and adsorption) during the second half of the experiments.

4. Conclusions

Non-disturbed batch and column experiments were carried out in this study with the aim of discerning the effect of sand co-presence on the efficiency of Cr^{VI} removal in Fe^0 - H_2O system. Batch experiments showed a minor increase in the removal efficiency of Cr^{VI} for the “ Fe^0 + sand” system with the lowest Fe^0 volumetric ratio (20%), compared

to “Fe⁰ + sand” systems with higher Fe⁰ volumetric ratios (50, 80%) and “Fe⁰ alone” system (100% Fe⁰). Column experiments revealed that mixing sand with Fe⁰ in the reactive zone results in shortening the period during which the column operates with no Cr^{VI} detected in the effluent. In spite of this fact, column tests confirmed the findings of batch experiments showing that the “Fe⁰ + sand” system exerted the highest efficiency in the removal of Cr^{VI} when the lowest Fe⁰ volumetric ratio (20% and 33.3% Fe⁰) was applied. Moreover, column experiments further revealed that the “Fe⁰ + sand” system with the lowest Fe⁰ volumetric ratio displayed better Cr^{VI} removal efficiency than the “Fe⁰ alone” system (100% Fe⁰) at pH 6.5 and similar efficacy at pH 7.1. Thus, the co-presence of sand inside the column reactive zone exerts a positive effect on Cr^{VI} removal efficiency, which increases with decreasing pH below neutral. This behavior was ascribed to capacity of the “Fe⁰ + sand” system to sustain the corrosion process of Fe⁰ and to generate higher amounts of secondary adsorbents/reductants for Cr^{VI} removal. Based on the outcomes of the present study, we suggest that abatement of Cr^{VI} water pollution should be conducted using filters having a volumetric ratio Fe⁰:sand = 1:3. The present result corroborates those of Bilardi et al. [18] and Btatkeu et al. [8] who identified an Fe⁰ volumetric ratio of 25% as optimal for the removal of cationic pollutants (Cu^{II}, Ni^{II}, Zn^{II}, methylene blue) in Fe⁰-H₂O system amended with non-expansive additives (sand, pumice).

Supplementary Materials: The following supporting information can be downloaded at: <https://www.mdpi.com/article/10.3390/w15040777/s1>. Figure S1. SEM micrograph of fresh Fe⁰ at different magnifications; Figure S2. SEM micrograph of exhausted Fe⁰ from 100% Fe⁰ system at different magnifications; Figure S3. SEM micrograph of exhausted Fe⁰ from 50% Fe⁰ system at different magnifications; Figure S4. SEM micrograph of exhausted Fe⁰ from 20% Fe⁰ system at different magnifications; Figure S5. EDX pattern of fresh Fe⁰; Figure S6. EDX pattern of exhausted Fe⁰ from “Fe⁰ only” system; Figure S7. EDX pattern of exhausted Fe⁰ from “50% Fe⁰ + 50% sand” system; Figure S8. EDX pattern of exhausted Fe⁰ from “20% Fe⁰ + 80% sand” system; Figure S9. XRD pattern of fresh Fe⁰; Figure S10. XRD pattern of exhausted Fe⁰ from 100% Fe⁰ system; Figure S11. XRD pattern of exhausted Fe⁰ from 50% Fe⁰ system; Figure S12. XRD pattern of exhausted Fe⁰ from 20% Fe⁰ system; Figure S13. Profiles of Cr^{VI} removal efficiencies for non-disturbed batch experiments, after 40 experimental days.; Figure S14. Evolution of Cr^{VI} breakthrough at pH 6.5, for columns having fixed Fe⁰ volume and variable total reactive zone volume V₂.; Figure S15. Evolution of Cr^{VI} breakthrough at pH 7.1, for columns having fixed Fe⁰ volume and variable total reactive zone volume V₂.; Figure S16. Evolution of Cr^{VI} breakthrough, for columns having variable Fe⁰ volume and fixed total reactive zone volume V₂.

Author Contributions: Conceptualization, M.G. and I.B.; methodology, M.G. and I.B.; software, M.G.; validation, M.G. and I.B.; formal analysis, M.G. and I.B.; investigation, M.G. and I.B.; resources, M.G. and I.B.; data curation, M.G. and I.B.; writing—original draft preparation, M.G.; writing—review and editing, M.G.; visualization, M.G. and I.B.; supervision, M.G. All authors have read and agreed to the published version of the manuscript.

Funding: This research received no external funding.

Data Availability Statement: Not applicable.

Acknowledgments: We sincerely thank the four anonymous reviewers from Water, whose insightful comments and suggestions provided on earlier version of this manuscript helped improve and clarify this study.

Conflicts of Interest: The authors declare no conflict of interest.

References

1. Mwakabona, H.T.; Nde-Tchoupe, A.I.; Njau, K.N.; Noubactep, C.; Wydra, K.D. Metallic iron for safe drinking water provision: Considering a lost knowledge. *Water Res.* **2017**, *117*, 127–142. [[CrossRef](#)] [[PubMed](#)]
2. Noubactep, C. Metallic iron for environmental remediation: A review of reviews. *Water Res.* **2015**, *85*, 114–123. [[CrossRef](#)] [[PubMed](#)]
3. Sun, Y.; Li, J.; Huang, T.; Guan, X. The influences of iron characteristics, operating conditions and solution chemistry on contaminants removal by zero-valent iron: A review. *Water Res.* **2016**, *100*, 277–295. [[CrossRef](#)] [[PubMed](#)]
4. Hu, R.; Cui, X.; Gwenzi, W.; Wu, S.; Noubactep, C. Fe⁰/H₂O systems for environmental remediation: The scientific history and future research directions. *Water* **2018**, *10*, 1739. [[CrossRef](#)]

5. Fu, F.; Dionysiou, D.D.; Liu, H. The use of zero-valent iron for groundwater remediation and wastewater treatment: A review. *J. Hazard. Mater.* **2014**, *267*, 94–205. [[CrossRef](#)] [[PubMed](#)]
6. Lipczynska-Kochany, E.; Harms, S.; Milburn, R.; Sprah, G.; Nadarajah, N. Degradation of carbon tetrachloride in the presence of iron and sulphur containing compounds. *Chemosphere* **1994**, *29*, 1477–1489. [[CrossRef](#)]
7. Ansaf, K.V.K.; Ambika, S.; Nambi, I.M. Performance enhancement of zero valent iron based systems using depassivators: Optimization and kinetic mechanisms. *Water Res.* **2016**, *102*, 436–444. [[CrossRef](#)]
8. Btatkeu-K, B.D.; Olvera-Vargas, H.; Tchatchueng, J.B.; Noubactep, C.; Caré, S. Determining the optimum Fe⁰ ratio for sustainable granular Fe⁰/sand water filters. *Chem. Eng. J.* **2014**, *247*, 265–274. [[CrossRef](#)]
9. Guan, X.; Sun, Y.; Qin, H.; Li, J.; Lo, I.M.C.; He, D.; Dong, H. The limitations of applying zero-valent iron technology in contaminants sequestration and the corresponding countermeasures: The development in zero-valent iron technology in the last two decades (1994–2014). *Water Res.* **2015**, *75*, 224–248. [[CrossRef](#)]
10. Madaffari, M.G.; Bilardi, S.; Calabro, P.S.; Moraci, N. Nickel removal by zero valent iron/lapillus mixtures in column systems. *Soils Found.* **2017**, *57*, 745–759. [[CrossRef](#)]
11. Noubactep, C.; Care, S.; Togue-Kamga, F.; Schöner, A.; Woafu, P. Extending service life of household water filters by mixing metallic iron with sand. *Clean Soil Air Water* **2010**, *38*, 951–959. [[CrossRef](#)]
12. Care, S.; Crane, R.; Calabro, P.S.; Ghauch, A.; Temgoua, E.; Noubactep, C. Modeling the permeability loss of metallic iron water filtration systems. *Clean Soil Air Water* **2013**, *41*, 275–282. [[CrossRef](#)]
13. Tao, R.; Yang, H.; Cui, X.; Xiao, M.; Gatcha-Bandjun, N.; Kenmogne-Tchidjo, J.F.; Lufingo, M.; Amoah, B.K.; Tepong-Tsindé, R.; Ndé-Tchoupé, A.I.; et al. The suitability of hybrid Fe⁰/aggregate filtration systems for water treatment. *Water* **2022**, *14*, 260. [[CrossRef](#)]
14. Miyajima, K.; Noubactep, C. Effects of mixing granular iron with sand on the efficiency of methylene blue discoloration. *Chem. Eng. J.* **2012**, *200–202*, 433–438. [[CrossRef](#)]
15. Noubactep, C. On the suitability of admixing sand to metallic iron for water treatment. *Int. J. Environ. Poll. Solut.* **2013**, *1*, 22–36. [[CrossRef](#)]
16. Ndé-Tchoupé, A.I.; Makota, S.; Nassi, A.; Rui, H.; Noubactep, C. The suitability of pozzolan as admixing aggregate for Fe⁰-based filters. *Water* **2018**, *10*, 417. [[CrossRef](#)]
17. O'Hannesin, S.F.; Gillham, R.W. Long-term performance of an in situ “iron wall” for remediation of VOCs. *Ground Water* **1998**, *36*, 164–170. [[CrossRef](#)]
18. Bilardi, S.; Calabro, P.S.; Care, S.; Moraci, N.; Noubactep, C. Improving the sustainability of granular iron/pumice systems for water treatment. *J. Environ. Manag.* **2013**, *121*, 133–141. [[CrossRef](#)]
19. Ebelle, T.C.; Makota, S.N.; Tepong-Tsindé, R.; Nassi, A.; Noubactep, C. Metallic iron and the dialogue of the deaf. *Fres. Environ. Bull.* **2019**, *28*, 8331–8340.
20. Hu, R.; Gwenzi, W.; Sipowo-Tala, V.R.; Noubactep, C. Water treatment using metallic iron: A tutorial review. *Processes* **2019**, *7*, 622. [[CrossRef](#)]
21. Cantrell, K.J.; Kaplan, D.I.; Wietsma, T.W. Zero-valent iron for the in situ remediation of selected metals in groundwater. *J. Hazard. Mater.* **1995**, *42*, 201–212. [[CrossRef](#)]
22. Blowes, D.W.; Ptacek, C.J.; Jambor, J.L. In-situ remediation of chromate contaminated groundwater using permeable reactive walls: Laboratory Studies. *Environ. Sci. Technol.* **1997**, *31*, 3348–3357. [[CrossRef](#)]
23. Melitas, N.; Chufe-Moscoso, O.; Farrell, J. Kinetics of soluble chromium removal from contaminated water by zerovalent iron media: Corrosion inhibition and passive oxide effects. *Environ. Sci. Technol.* **2001**, *35*, 3948–3953. [[CrossRef](#)] [[PubMed](#)]
24. Junyapoon, S.; Weerapong, S. Removal of hexavalent chromium from aqueous solutions by scrap iron fillings. *KMITL Sci. Technol. J.* **2006**, *6*, 1–12.
25. Gheju, M.; Iovi, A. Kinetics of hexavalent chromium reduction by scrap iron. *J. Hazard. Mater.* **2006**, *B135*, 66–73. [[CrossRef](#)] [[PubMed](#)]
26. Yang, J.E.; Kim, J.S.; Ok, Y.S.; Kim, S.J.; Yoo, K.Y. Capacity of Cr(VI) reduction in an aqueous solution using different sources of zerovalent irons. *Korean J. Chem. Eng.* **2006**, *23*, 935–939. [[CrossRef](#)]
27. Qian, H.; Wu, Y.; Liu, Y.; Xu, X. Kinetics of hexavalent chromium reduction by iron metal. *Front. Environ. Sci. Engin. China* **2008**, *2*, 51–56. [[CrossRef](#)]
28. Hou, M.; Wan, H.; Liu, T.; Fan, Y.; Liu, X.; Wang, X. The effect of different divalent cations on the reduction of hexavalent chromium by zerovalent iron. *Appl. Catal. B* **2008**, *84*, 170–175. [[CrossRef](#)]
29. Geng, B.; Jin, Z.; Li, T.; Qi, X. Kinetics of hexavalent chromium removal from water by chitosan-Fe⁰ nanoparticles. *Chemosphere* **2009**, *75*, 825–830. [[CrossRef](#)]
30. Franco, D.V.; Da Silva, L.M.; Jardim, W.F. Chemical reduction of hexavalent chromium and its immobilisation under batch conditions using a slurry reactor. *Water Air Soil Pollut.* **2009**, *203*, 305–315. [[CrossRef](#)]
31. Dutta, R.; Mohammad, S.K.S.; Chakrabarti, S.; Chaudhuri, B.; Bhattacharjee, S.; Dutta, B.K. Reduction of hexavalent chromium in aqueous medium with zerovalent iron. *Water Environ. Res.* **2010**, *82*, 138–146. [[CrossRef](#)]
32. Fiuza, A.; Silva, A.; Carvalho, G.; de la Fuente, A.V.; Delerue-Matos, C. Heterogeneous kinetics of the reduction of chromium (VI) by elemental iron. *J. Hazard. Mater.* **2010**, *175*, 1042–1047. [[CrossRef](#)] [[PubMed](#)]
33. Lee, J.W.; Cha, D.K.; Oh, Y.K.; Ko, K.B.; Jin, S.H. Wastewater screening method for evaluating applicability of zero-valent iron to industrial wastewater. *J. Hazard. Mater.* **2010**, *180*, 354–360. [[CrossRef](#)] [[PubMed](#)]

34. Alidokht, L.; Khataee, A.R.; Reyhanitabar, A.; Oustan, S. Reductive removal of Cr(VI) by starch-stabilized Fe⁰ nanoparticles in aqueous solution. *Desalination* **2011**, *270*, 105–110. [[CrossRef](#)]
35. Jiao, C.; Cheng, Y.; Fan, W.; Li, J. Synthesis of agar-stabilized nanoscale zero-valent iron particles and removal study of hexavalent chromium. *Int. J. Environ. Sci. Technol.* **2015**, *12*, 1603–1612. [[CrossRef](#)]
36. Li, J.; Qin, H.; Zhang, W.X.; Shi, Z.; Zhao, D.; Guan, X. Enhanced Cr(VI) removal by zero-valent iron coupled with weak magnetic field: Role of magnetic gradient force. *Sep. Purif. Technol.* **2017**, *176*, 40–47. [[CrossRef](#)]
37. Liu, J.; Mwamulima, T.; Wang, Y.; Fang, Y.; Song, S.; Peng, C. Removal of Pb(II) and Cr(VI) from aqueous solutions using the fly ash-based adsorbent material-supported zero-valent iron. *J. Molec. Liq.* **2017**, *243*, 205–211. [[CrossRef](#)]
38. Huang, X.Y.; Ling, L.; Zhang, W.X. Nanoencapsulation of hexavalent chromium with nanoscale zero-valent iron: High resolution chemical mapping of the passivation layer. *J. Environ. Sci.* **2018**, *67*, 4–13. [[CrossRef](#)]
39. Zhang, Y.; Gao, X.; Xu, C. The sequestration of Cr(VI) by zero valent iron under a non-uniform magnetic field: An interfacial dynamic reaction. *Chemosphere* **2020**, *249*, 126057. [[CrossRef](#)]
40. Rong, K.; Wang, J.; Zhang, Z.; Zhang, Z. Green synthesis of iron nanoparticles using Korla fragrant pear peel extracts for the removal of aqueous Cr(VI). *Ecol. Eng.* **2020**, *149*, 105793. [[CrossRef](#)]
41. Miyajima, K.; Noubactep, C. Characterizing the impact of sand addition on the efficiency of granular iron for contaminant removal in batch systems. *Chem. Eng. J.* **2015**, *262*, 891–896. [[CrossRef](#)]
42. Ndé-Tchoupé, A.I.; Nansou-Njiki, C.P.; Hu, R.; Nassi, A.; Noubactep, C.; Licha, T. Characterizing the reactivity of metallic iron for water defluoridation in batch studies. *Chemosphere* **2019**, *219*, 855–863. [[CrossRef](#)] [[PubMed](#)]
43. Westerhoff, P.; James, J. Nitrate removal in zero-valent iron packed columns. *Water Res.* **2003**, *37*, 1818–1830. [[CrossRef](#)] [[PubMed](#)]
44. Hussam, A. Contending with a development disaster: SONO filters remove arsenic from well water in Bangladesh. *Innovations* **2009**, *4*, 89–102. [[CrossRef](#)]
45. Ahmed, J.U.; Tinne, W.S.; Al-Amin, M.; Rahanaz, M. Social innovation and SONO filter for drinking water. *Soc. Busin. Rev.* **2018**, *13*, 15–26. [[CrossRef](#)]
46. Kaplan, D.I.; Gilmore, T.J. Zerovalent iron removal rates of aqueous Cr(VI) measured under flow conditions. *Water Air Soil Pollut.* **2004**, *155*, 21–33. [[CrossRef](#)]
47. Gheju, M.; Balcu, I. Sustaining the efficiency of the Fe(0)/H₂O system for Cr(VI) removal by MnO₂ amendment. *Chemosphere* **2019**, *214*, 389–398. [[CrossRef](#)]
48. Flury, B.; Eggenberger, U.; Mader, U. First results of operating and monitoring an innovative design of a permeable reactive barrier for the remediation of chromate contaminated groundwater. *J. Appl. Geochem.* **2009**, *24*, 687–697. [[CrossRef](#)]
49. Ishikawa, Y.; Saitoh, O.; Numabe, A. Estimation of long-term changes in Cr(VI) concentration in public water after countermeasures against water pollution. *J. Japan Soc. Water Environ.* **2004**, *27*, 423–429. [[CrossRef](#)]
50. APHA; AWWA; WEF. 3500-Cr B; Colorimetric method. In *Standard Methods for the Examination of Water and Wastewater*, 21st ed.; Eaton, A.D., Clesceri, L.S., Rice, E.W., Greenberg, A.E., Franson, M.A.H., Eds.; American Public Health Association: Washington, DC, USA, 2005; pp. 3.67–3.68.
51. APHA; AWWA; WEF. 3500-Fe B; Phenantroline method. In *Standard Methods for the Examination of Water and Wastewater*, 21st ed.; Eaton, A.D., Clesceri, L.S., Rice, E.W., Greenberg, A.E., Franson, M.A.H., Eds.; American Public Health Association: Washington, DC, USA, 2005; pp. 3.77–3.78.
52. Dai, Y.; Hua, Y.; Jiang, B.; Zou, J.; Tian, G.; Fu, H. Carbothermal synthesis of ordered mesoporous carbon-supported nano zero-valent iron with enhanced stability and activity for hexavalent chromium reduction. *J. Hazard. Mater.* **2016**, *309*, 249–258. [[CrossRef](#)]
53. Papassiopi, N.; Vaxevanidou, K.; Christou, C.; Karagianni, E.; Antipas, G.S.E. Synthesis, characterization and stability of Cr(III) and Fe(III)hydroxides. *J. Hazard. Mater.* **2014**, *264*, 490–497. [[CrossRef](#)] [[PubMed](#)]
54. Gheju, M. Decontamination of hexavalent chromium-polluted waters: Significance of metallic iron technology. In *Enhancing Cleanup of Environmental Pollutants. Non Biological Approaches*; Anjum, N., Gill, S., Tuteja, N., Eds.; Springer International Publishing: Cham, Switzerland, 2017; Volume 2, pp. 209–254.
55. Bilardi, S.; Calabro, P.S.; Care, S.; Moraci, N.; Noubactep, C. Effect of pumice and sand on the sustainability of granular iron beds for the aqueous removal of Cu^{II}, Ni^{II}, and Zn^{II}. *Clean Soil Air Water* **2013**, *41*, 835–843. [[CrossRef](#)]
56. Gatcha-Bandjun, N.; Noubactep, C.; Loura, B.B. Mitigation of contamination in effluents by metallic iron: The role of iron corrosion products. *Environ. Technol. Innovat.* **2017**, *8*, 71–83. [[CrossRef](#)]
57. Domga, R.; Togue-Kamga, F.; Noubactep, C.; Tchatchueng, J.B. Discussing porosity loss of Fe⁰ packed water filters at ground level. *Chem. Eng. J.* **2015**, *263*, 127–134. [[CrossRef](#)]
58. Noubactep, C.; Care, S. Dimensioning metallic iron beds for efficient contaminant removal. *Chem. Eng. J.* **2010**, *163*, 454–460. [[CrossRef](#)]
59. Buerge, I.J.; Hug, S.J. Kinetics and pH dependence of chromium(VI) reduction by iron(II). *Environ. Sci. Technol.* **1997**, *31*, 1426–1432. [[CrossRef](#)]
60. Fendorf, S.E.; Li, G. Kinetics of chromate reduction by ferrous iron. *Environ. Sci. Technol.* **1996**, *30*, 1614–1617. [[CrossRef](#)]
61. Schlautman, M.A.; Han, I. Effects of pH and dissolved oxygen on the reduction of hexavalent chromium by dissolved ferrous iron in poorly buffered aqueous systems. *Water Res.* **2001**, *35*, 1534–1546. [[CrossRef](#)]

62. Eary, L.E.; Rai, D. Chromate removal from aqueous wastes by reduction with ferrous iron. *Environ. Sci. Technol.* **1988**, *22*, 972–977. [[CrossRef](#)]
63. Konadu-Amoah, B.; Hu, R.; Nde-Tchoupe, A.I.; Gwenzi, W.; Noubactep, C. Metallic iron (Fe⁰)-based materials for aqueous phosphate removal: A critical review. *J. Environ. Manag.* **2022**, *315*, 115–157. [[CrossRef](#)]
64. Firdous, R.; Devlin, J.F. Visualizations and optimization of iron-sand mixtures for permeable reactive barriers. *Ground Water Monit. Remed.* **2015**, *35*, 78–84. [[CrossRef](#)]
65. Oh, Y.J.; Song, H.; Shin, W.S.; Choi, S.J.; Kim, Y.H. Effect of amorphous silica and silica sand on removal of chromium(VI) by zero-valent iron. *Chemosphere* **2007**, *66*, 858–865. [[CrossRef](#)] [[PubMed](#)]
66. White, A.F.; Paterson, M.L. Reduction of aqueous transition metal species on the surface of Fe(II)-containing oxides. *Geochim. Cosmochim. Acta.* **1996**, *60*, 3799–3814. [[CrossRef](#)]
67. Tomaszewski, E.J.; Lee, S.; Rudolph, J.; Xu, H.; Ginder-Vogel, M. The reactivity of Fe(II) associated with goethite formed during short redox cycles toward Cr(VI) reduction under oxic conditions. *Chem. Geol.* **2017**, *464*, 101–109. [[CrossRef](#)]
68. Buerge, I.J.; Hug, S.J. Influence of mineral surfaces on chromium(VI) reduction by iron(II). *Environ. Sci. Technol.* **1999**, *33*, 4285–4291. [[CrossRef](#)]
69. Nelson, J.; Joe-Wong, C.; Maher, K. Cr(VI) reduction by Fe(II) sorbed to silica surfaces. *Chemosphere* **2019**, *234*, 98–107. [[CrossRef](#)]
70. Nanseu-Njiki, C.P.; Gwenzi, W.; Pengou, M.; Rahman, M.A.; Noubactep, C. Fe⁰/H₂O Filtration systems for decentralized safe drinking water: Where to from here? *Water* **2019**, *11*, 429. [[CrossRef](#)]
71. Xiao, M.; Hu, R.; Ndé-Tchoupé, A.I.; Gwenzi, W.; Noubactep, C. Metallic iron for water remediation: Plenty of room for collaboration and convergence to advance the science. *Water* **2022**, *14*, 1492. [[CrossRef](#)]
72. Lu, Y.W.; Huang, C.P.; Huang, Y.H.; Lin, C.P.; Chen, H.T. Effect of pH on the oxidation of ferrous ion and immobilization technology of iron hydr(oxide) in fluidized bed reactor. *Sep. Sci. Technol.* **2008**, *43*, 1632–1641. [[CrossRef](#)]
73. Sharma, S.K.; Greetham, M.R.; Schippers, J.C. Adsorption of iron(II) onto filter media. *J. Water SRT-Aqua.* **1999**, *48*, 84–91.
74. Buamah, R.; Petrushevski, B.; Schippers, J.C. Oxidation of adsorbed ferrous iron: Kinetics and influence of process conditions. *Water Sci. Technol.* **2009**, *60*, 2353–2363. [[CrossRef](#)] [[PubMed](#)]
75. Mettler, S.; Wolthers, M.; Charlet, L.; von Gunten, U. Sorption and catalytic oxidation of Fe(II) at the surface of calcite. *Geochim. Cosmochim. Acta* **2009**, *73*, 1826–1840. [[CrossRef](#)]

Disclaimer/Publisher’s Note: The statements, opinions and data contained in all publications are solely those of the individual author(s) and contributor(s) and not of MDPI and/or the editor(s). MDPI and/or the editor(s) disclaim responsibility for any injury to people or property resulting from any ideas, methods, instructions or products referred to in the content.